Review Article

Zhanlong Piao, Liguang Zhu*, Xingjuan Wang, Zengxun Liu, Hebin Jin, Xiaoshi Zhang, Quanli Wang, and Chao Kong

Exploitation of Mold Flux for the Ti-bearing Welding Wire Steel ER80-G

https://doi.org/10.1515/htmp-2019-0040
Received Mar 13, 2019; accepted Jul 17, 2019

Abstract: In order to improve the surface defects of strand, the mold flux is exploited for the Ti-bearing welding wire steel ER80-G. The composition of mold flux is designed by analyzing the solidification characteristics of ER80-G and the slag system isothermal section diagram, simulating by the FactSage thermodynamics software. The Ti-bearing welding wire steel ER80-G belongs to the peritectic steel. The melting point range of the newly designed mold flux system is from 1030°C to 1129°C, the melting rate range is from 58 s to 64 s, the viscosity range at the temperature of 1300°C is from 0.33 Pa·s to 0.50 Pa·s, the crystallization temperature range is from 1160°C to 1293°C, the crystalline fraction range is from 34% to 85%. The surface defects of strand which transverse depression, longitudinal depression, slag runner and so on were obviously improved when the newly design mold flux F3, F5, F9 were used to the production respectively. Those results suggest that 0.9 basicity with 28.4%-CaO, 31.6%-SiO_2, 3%-MgO, 10%-Na_2O, 10%-CaF_2, 6%-Al_2O_3, 1%-Fe_2O_3, 10%-T_c and all groups with 1.0 and 1.1 basicity show the best properties for Ti-bearing welding wire steel ER80-G.

Keywords: Ti-bearing welding wire steel ER80-G; newly designed mold flux; peritectic reaction; FactSage simulation

1 Introduction

The TiN was from the combination of [Ti] and [N] plays a role in nitrogen fixation for the Ti-bearing welding wire steel ER80-G, which improves the ability of weld metal to resist nitrogen gas holes and reduces spatter 30% to 50%. This steel is widely applied in the welding field, such as automobiles, ships, bridges and other steel structure [1–5]. But the difficulty of continuous casting is resulted from nozzle blocking and cold steel, and there are a lot of surface defects of strand, such as transverse depression, longitudinal depression, slag runner and slag pit and so on.

The Ti-bearing welding wire steel invented firstly in Japan had less spatter and better deposited property, and then it was extensive popularization [6, 7]. Shagang [9], qinggang [10], tanggang [11] and taigang [12] had produced Ti-bearing welding wire steel, who overcome the problem of nozzle blocking and cold steel through the optimization of the relation of [Al]-[Ti]-[O]-[N] and process parameters. But the researches about the surface defects of Ti-bearing welding wire steel ER80-G are relatively few. The surface quality is closely related to the properties of mold flux, if the viscosity and melting point is high, which will result that the liquid flux layer become thinner and then the sintered layer and powder layer are easier to flow into the gap when the mold oscillated, meanwhile the liquid flux layer

***Corresponding Author: Liguang Zhu:** Hebei High Quality Steel Continuous Casting Engineering Technology Research Center, College of Metallurgy and Energy, North China University of Science and Technology, Tangshan, 063000, China; Email: zhuliguang@ncst.edu.cn
Zhanlong Piao: School of Metallurgical and Ecological Engineering, University of Science and Technology Beijing, Beijing 100083, China; Email: zhanlongP_ncst@163.com
Xingjuan Wang: Hebei High Quality Steel Continuous Casting Engineering Technology Research Center, College of Metallurgy and Energy, North China University of Science and Technology, Tangshan, 063000, China; Email: wxingjuan@ncst.edu.cn
Zengxun Liu: Hebei High Quality Steel Continuous Casting Engineering Technology Research Center, College of Metallurgy and Energy, North China University of Science and Technology, Tangshan, 063000, China; Email: liuzengxun@ncst.edu.cn
Hebin Jin: Hebei High Quality Steel Continuous Casting Engineering Technology Research Center, College of Metallurgy and Energy, North China University of Science and Technology, Tangshan, 063000, China; Email: 18716063795@163.com
Xiaoshi Zhang: Hebei High Quality Steel Continuous Casting Engineering Technology Research Center, College of Metallurgy and Energy, North China University of Science and Technology, Tangshan, 063000, China; Email: 1510053033@163.com
Quanli Wang: Wire Rod Department of HBIS Group Chengsteel Company; Email: wangquanli@hbisco.com
Chao Kong: Wire Rod Department of HBIS Group Chengsteel Company; Email: kongchao@hbisco.com

Table 1: Composition of the Ti-bearing welding wire steel ER80-G(wt%)

C	Si	Mn	S	P	Ni	Mo	Cr	Ti
0.07~0.09	0.40~0.50	1.50~1.60	≤ 0.015	≤ 0.02	1.60~1.75	0.30~0.45	0.35~0.45	0.05~0.07

Table 2: The specific components of original mold flux(wt%)

Flux	CaO	SiO_2	R	Al_2O_3	Fe_2O_3	Na_2O	CaF_2	MgO	Tc
F0	28.9	31.8	0.9	5.6	1	5	4.6	0.8	16

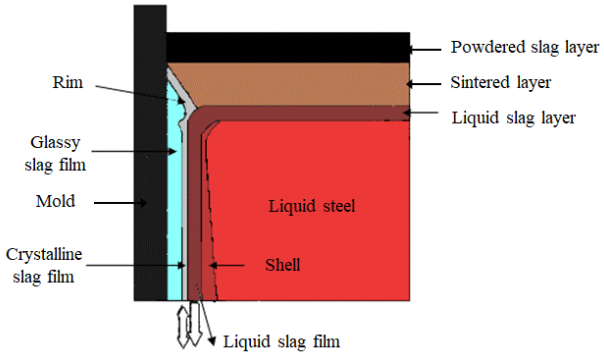

Figure 1: The schematic figure of mold flux structure

flowed unsteadily makes the heat-transfer nonuniformly, which may cause surface defects.

The mold flux for Ti-bearing welding wire steel ER80-G is special because of exciting the steel-slag interface reaction, [Ti] + (SiO_2) = (TiO_2) + [Si], which is occurred in the mold in continuous casting. It changes the content of mold fluxes, increases the basicity and the melting temperature, reduces the viscosity [13–18]. So the liquid slag layer is not stable, and then leads to poor lubrication and heat-transfer.

The mold flux plays an important role in the continuous casting, and its structure in the mold is illustrated in Figure 1. The liquid slag layer, sintered layer and powdered slag layer are over the surface of the molten steel, and the liquid slag film, crystalline film and glassy slag film are located between the mold wall and initial shell [19]. The liquid slag film acted as the lubrication can reduce the friction between the mold wall and the shell, the crystalline film can control the horizontal heat transfer of the shell [20–26].

According to the process parameters of Ti-bearing welding wire steel ER80-G, its solidification characteristics and the effect of components on the melting temperature and viscosity of slag system were simulated by FactSage thermodynamics software, and the viscosity obeyed the empirical formula, $\eta_{1300^\circ C} \cdot V_c$=0.5~0.7 [19], for the Ti-bearing welding wire steel ER80-G, which the casting section size was 165 mm×165 mm and the casting speed was 1.7 m/min, and then the composition of mold flux was designed. The relatively physical and chemical properties, melting characteristic, viscosity characteristic and crystallization characteristic were measured by the automatic tester slag melting point and melting speed, the brookfield rotary viscometer and the SHTT/DHTT. And then the component content of mold flux for Ti-bearing welding wire steel ER80-G was decided by analyzing the measured results, which had guidance significance in designing the mold flux.

2 Experimental Methods

The solidification characteristics of Ti-bearing welding wire steel ER80-G was simulated by the scheil solidification of "Equilib" module in FactSage software, the calculation temperature was set at 1530°C~1430°C for observing the solidification process at high temperature, the carbon content was set at 0~0.2% for studying the effect of the different carbon content on the solidification mode, and the composition were listed in Table 1.

The mold flux was exploited based on a commercial benchmark mold flux for the Ti-bearing welding wire steel ER80-G, the specific components were listed in Table 2. The F0 represented the original mold flux was CaO-SiO_2-Al_2O_3 traditional base slag system.

The design direction of mold flux was decided by the solidification characteristic of the Ti-bearing welding wire steel ER80-G. Meanwhile, the "phase diagram" module of FactSage software was used for simulating the ternary phase diagrams to analyze the effect of the component on the melting temperature of mold flux, and the "Equilib" module and "Viscosity" module of FactSage software were used for calculating the viscosity of mold flux at the temperature of 1300°C, and the Einstein-Roscoe Equation used in viscosity calculation of solid and liquid mixtures

was shown in equation 1. The component content range of mold flux was designed according to the simulated results of FactSage software.

$$\text{Viscosity}_{(solid+liquidmixture)} \approx \text{Viscosity}_{(liquid)} + (1 - \text{solid fraction})^{-2.5} \quad (1)$$

Where the $\text{Viscosity}_{(solid+liquidmixture)}$ is the calculated viscosity of mixtures, $\text{Viscosity}_{(liquid)}$ is the viscosity of liquid flux, which can be calculated from "Viscosity" module from mold flux component calculated from "Equilib" module; the solid fraction is the volume fraction of solid in mixtures, which can be calculated using "Equilib" module at given flux system composition.

The automatic tester slag melting point and melting speed was used to test the melting characteristic, its accuracy was ±3°C. A cylinder φ 3 mm×3 mm prepared by grinding the mold flux to 200 mesh was heated in the heating furnace, the height of the sample was observed during the melting process and the melting temperature was determined according to the industry standard (YB/T 186-2001) which was from China. The temperature at which the height of the sample become 3/4 of the original height is used as the softening temperature, the corresponding temperatures of 1/2 and 1/4 are respectively the melting point and flowing temperature of mold flux. Firstly, the K_2SO_4, the melting temperature is 1067°C, was used as the standard sample to judge the accuracy of the equipment. Secondly, the mold flux sample was tested three times with the difference between the highest test value and the lowest test value was less than 20°C, and then the corresponding temperature was obtained by calculating the average value of three test. If not, it will test again. The melting rate was expressed by the melting time of the sample tested at 1350°C, the sample was also tested three times and then calculated the average value of it. The schematic automatic tester slag melting point and melting speed was shown in Figure 2.

The viscosity of mold flux was tested by the Brookfield Rotary Viscometer. 300g carbon-free mold flux was put into the graphite crucible of φ 56 mm × 80 mm. It was heated in $MoSi_2$ furnace and heated to 1400°C for 10 min, which made the composition of mold powder uniformly. The viscosity was measured when the temperature down to 1300°C. The schematic of Brookfield Rotary Viscometer was shown in Figure 3.

The crystallization temperature and the crystalline fraction were measured by the SHTT/DHTT. Firstly, the sample was decarburized completely in the muffler furnace at 700°C. Secondly, the sample which must be mixed well was grinded to 200 mesh. Thirdly, the sample which

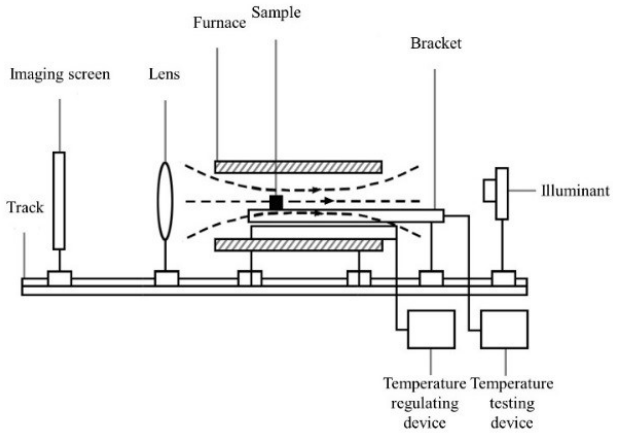

Figure 2: The schematic automatic tester slag melting point and melting speed

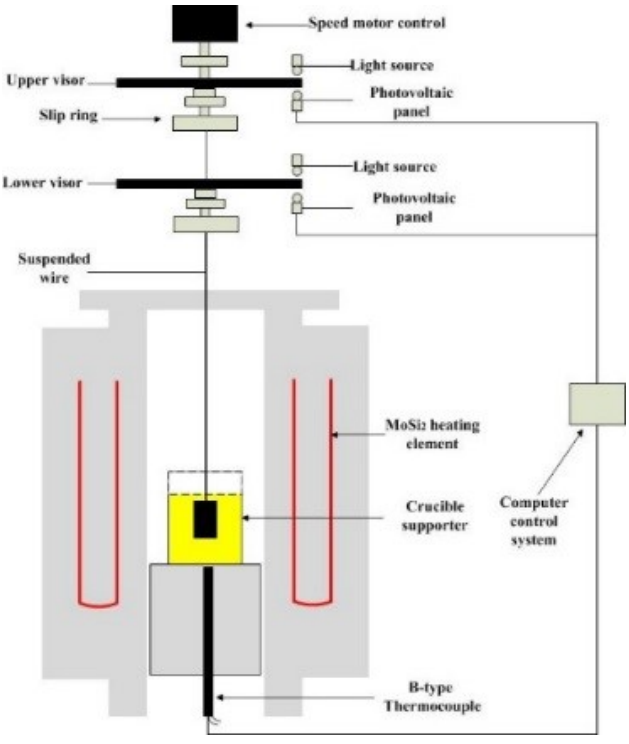

Figure 3: The schematic of brookfield rotary viscometer

was prepared into a paste with the anhydrous ethanol was mounted on a B type thermocouple with the specific temperature control system. The sample was heated to 1500°C at a rate of 10°C/s and kept for 5 minutes to eliminate bubbles and homogenize chemical composition, and it was tested with the cooling rate was 50°C/s. The K_2SO_4, the melting temperature is 1067°C, was used as the standard sample to judge the accuracy of the equipment before measuring the sample. The crystallization temperature of mold flux was achieved by calculating the average value of three

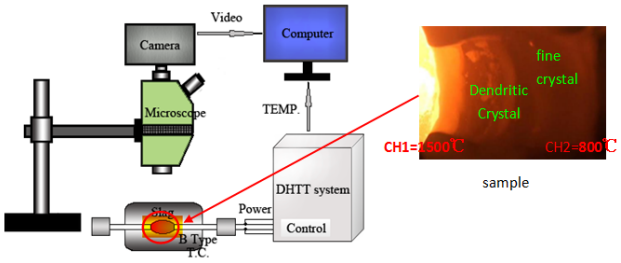

Figure 4: The schematic of SHTT/DHTT

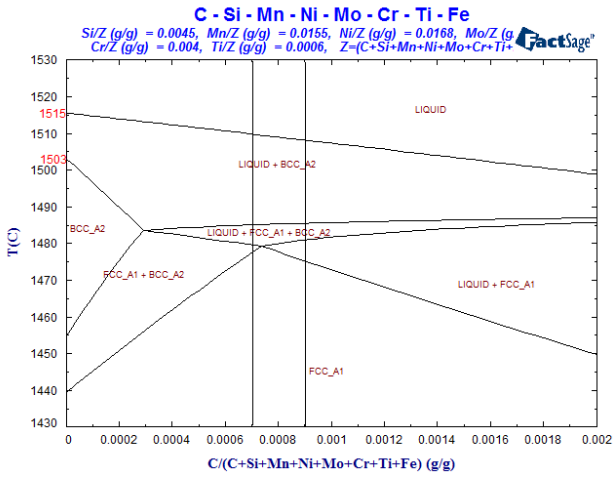

Figure 5: The solidification process of ER80-G on high temperature

times testing results whose difference was less than ±10°C, if not, it need to do it again. The crystalline fraction was calculated by the software. The schematic of SHTT/DHTT was shown in Figure 4.

3 Results and Discussion

3.1 The solidification characteristics

Figure 5 showed the solidification characteristics of the welding wire steel containing titanium ER80-G.

The liquidus temperature of the welding wire steel containing titanium ER80-G was about 1513°C. Its solidification mode was L→ L+δ→ L+γ+δ→ L+γ→ γ. The peritectic reaction, L+δ→ γ, appeared among 1490°C~1485°C, which was belong to peritectic steel. The compactness degree of the austenite which is a face-centered cubic structure is higher than the ferrite δ which is a body-centered cubic structure [27–29]. The volume of the strand shrunk sharply when the peritectic reaction occurred. If the mold flux did not flow evenly, the heat-transfer of the strand shell will be uneven, and the surface quality problem will be easily caused.

Heat-transfer Control should be considered in designing newly mold flux of Ti-bearing welding wire steel ER80-G. The horizontal heat-transfer of the initial strand shell at the meniscus can be controlled by adjusting the crystallization temperature and crystalline fraction of the mold flux [30]. Meanwhile, the viscosity, melting point and melting rate of the mold flux should be considered for ensuring the reasonable flow of the liquid flux layer and the good lubricating effect.

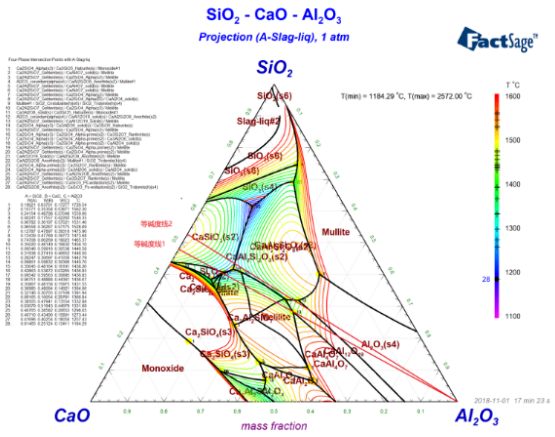

Figure 6: CaO-SiO_2-Al_2O_3 ternary phase diagram

3.2 The isothermal section phase diagram

Figure 6 showed the CaO-SiO_2-Al_2O_3 ternary phase diagram was calculated by the FactSage simulation software. The temperature was set at 1100°C~1600°C and the step length was 20°C in order to fit the actual production conditions.

The precipitation temperature range of mineral phase was from 1184°C to 1726°C the melting temperature of the region surrounded by blue curve was lower, about 1184°C~1298°C. There was a lower melting point region nearby number 28 corresponding to the lower basicity of the mold flux which was disadvantage for the control heat-transfer of strand shell. The low melting point region also appeared near the number 26 and 27 corresponding to the basicity range of the mold flux was among 0.9~1.1, which was shown by the isobaric curve 1 and 2. So the binary basicity of CaO-SiO_2-Al_2O_3 slag system was designed at 0.9~1.1.

The effects of different contents of CaF_2, Na_2O and MgO on the melting temperature and viscosity of CaO-SiO_2-

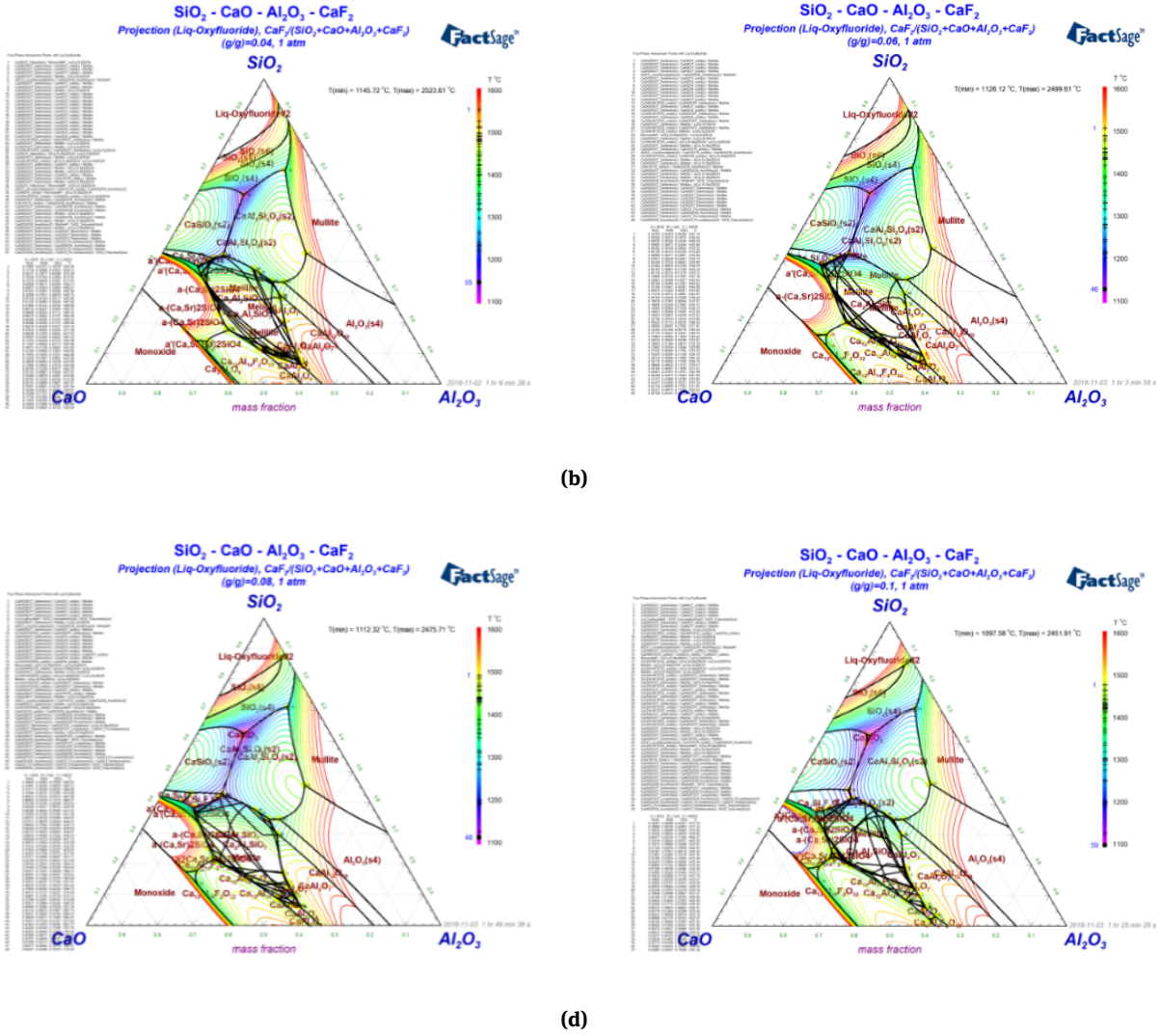

Figure 7: The isothermal section of the CaO-SiO_2-Al_2O_3 ternary slag system with the content of CaF_2 is 4%, 6%, 8% and 10%

Al_2O_3 ternary slag system were calculated by the FactSage software, and the optimum content range of them was studied out.

Figure 7 showed the isothermal section of the CaO-SiO_2-Al_2O_3 ternary slag system with the content of CaF_2 was 4%, 6%, 8% and 10%.

The temperature of blue isotherm curve was about 1250°C, which was the low melting point region, and the temperature of isotherm curve increased orderly from inside to outside. The low melting point region increased gradually with the increase of CaF_2, which suggested that the CaF_2 could significantly reduce the melting temperature of mold flux. Long *et al.* [31] considered that CaF_2 which was less than 12% could obviously decrease the melting temperature of high basicity mold flux. Wang *et al.* [32] found that B_2O_3 and CaF_2 could reduce the melting temperature, so did the viscosity. So the CaF_2 content range was designed at 4%~10%.

Figure 8 showed the isothermal section of the CaO-SiO_2-Al_2O_3 ternary slag system with the content of MgO was 2%, 4%, 6% and 8%.

With the content of MgO increased, the low melting point region moves to low basicity, the melting temperature increases and the crystallization regions of wollastonite and clinopyroxene gradually expanses. When the basicity was 0.9~1.1 and MgO content was 2%, there was a low melting point region. Wang *et al.* [33] found that increasing 1%MgO will increase the melting temperature by about 20°C when the MgO content was among 2%~8%. So the MgO content was designed at 1%~3%.

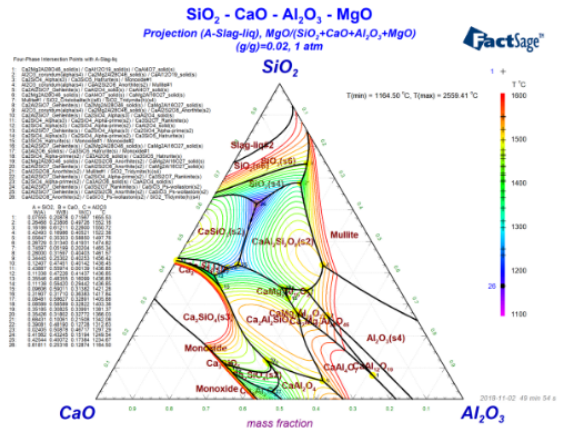

(a)

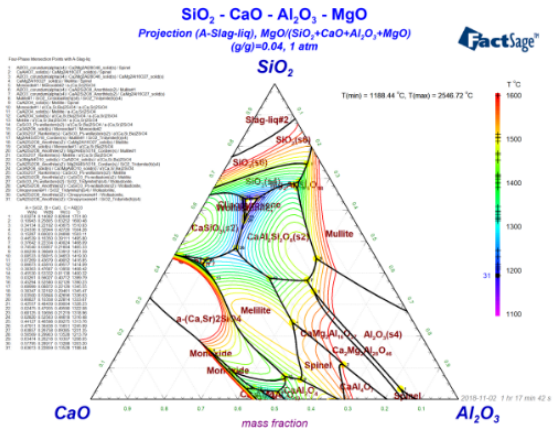

(b)

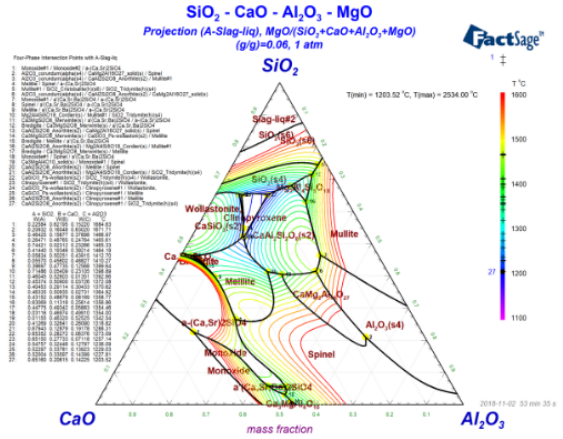

(c)

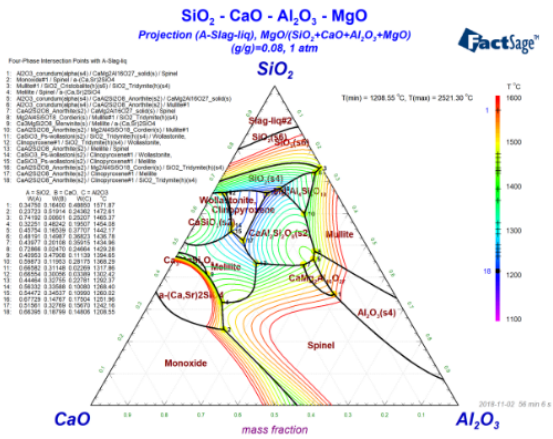

(d)

Figure 8: The isothermal section of the CaO-SiO_2-Al_2O_3 ternary slag system with the content of MgO is 2%, 4%, 6% and 8%

Figure 9 showed the isothermal section of the CaO-SiO_2-Al_2O_3 ternary slag system with the content of Na_2O was 5%, 7%, 9% and 11%.

With the Na_2O content increased, the low melting point region enlarges gradually and its temperature decreases from 1130°C to 994°C. Na_2O could reduce obviously the melting temperature, so the composition of CaO-SiO_2-Al_2O_3 slag system could be adjusted in a wide range. The researches confirmed the result [31, 34, 35]. So the Na_2O content was designed at 5%~11%.

The viscosity of mold flux with different contents of MgO, Na_2O, CaF_2 were computed by the "Equilib" model and "Viscosity" model of FactSage software. Figure 10 showed variation curve of component content and viscosity which was drew by Origin software.

With the content of MgO, Na_2O, CaF_2 increased, the mold flux viscosity is reduced. However, the degree of viscosity reduction was different among the three components, and the order of their ability to reduce viscosity was CaF_2>Na_2>MgO.

In summary, the base slag system of mold flux was proposed as CaO-SiO_2-Al_2O_3 ternary slag system, and the basicity was 0.9~1.1. The content of MgO was 1%~3%, the content of Na_2O was 6%~10%, the content of CaF_2 was 8%~10%, the content of Al_2O_3 was 6% and the content of Fe_2O_3 was 1%. The carbon material whose content was 10% was made up graphite and carbon black, and the ratio of them was 2:1. F1~F9 was the newly design of nine groups of CaO-SiO_2-Al_2O_3 slag system. The specific components were listed in Table 3.

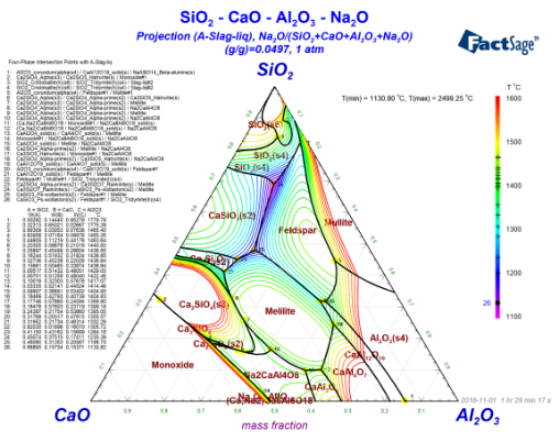

(a)

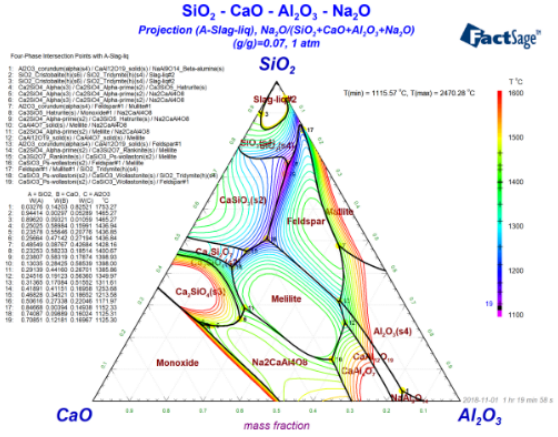

(b)

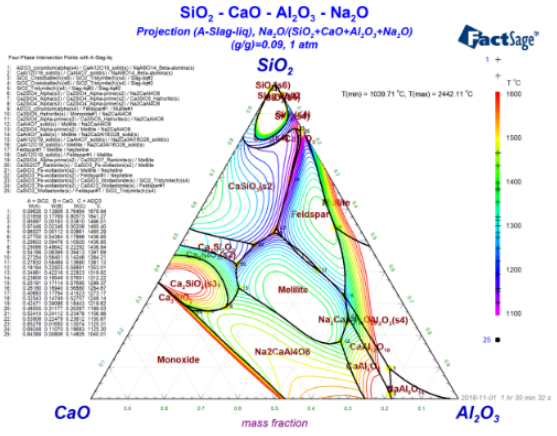

(c)

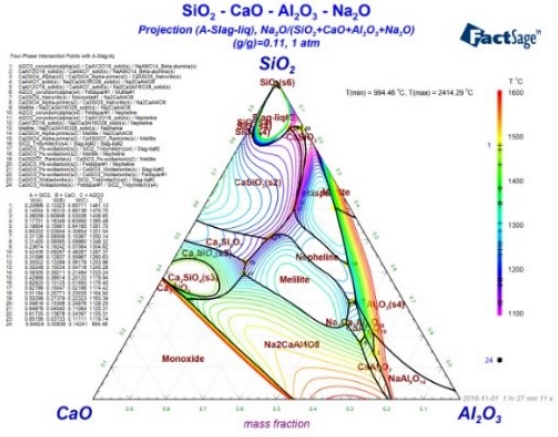

(d)

Figure 9: The isothermal section of the CaO-SiO_2-Al_2O_3 ternary slag system with the content of Na_2O is 5%, 7%, 9% and 11%

Table 3: The specific components of mold fluxes (wt%)

level	element								
	CaO	SiO_2	R	Al_2O_3	Fe_2O_3	Na_2O	CaF_2	MgO	Tc
F1	32.2	35.8	0.9	6	1	6	8	1	10
F2	30.3	33.7	0.9	6	1	8	9	2	10
F3	28.4	31.6	0.9	6	1	10	10	3	10
F4	32.5	32.5	1.0	6	1	6	10	2	10
F5	32	32	1.0	6	1	8	8	3	10
F6	31.5	31.5	1.0	6	1	10	9	1	10
F7	33	31	1.1	6	1	6	9	3	10
F8	33.5	30.5	1.1	6	1	8	10	1	10
F9	33	30	1.1	6	1	10	8	2	10

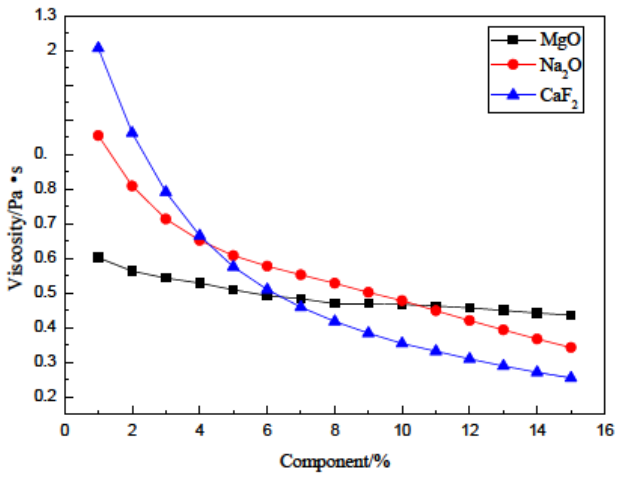

Figure 10: The variation curve of component content and viscosity

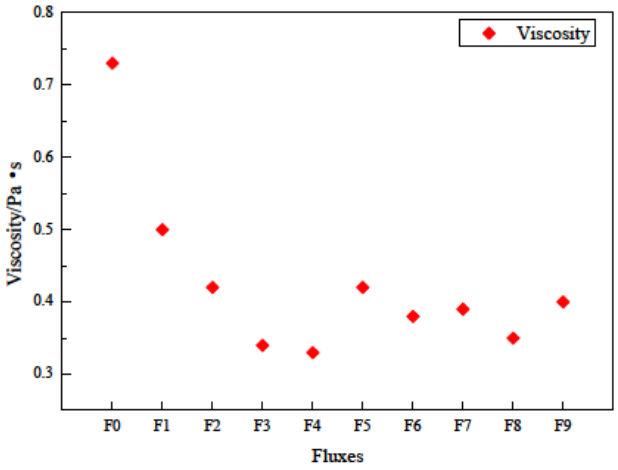

Figure 12: The viscosity of fluxes 0 through 10

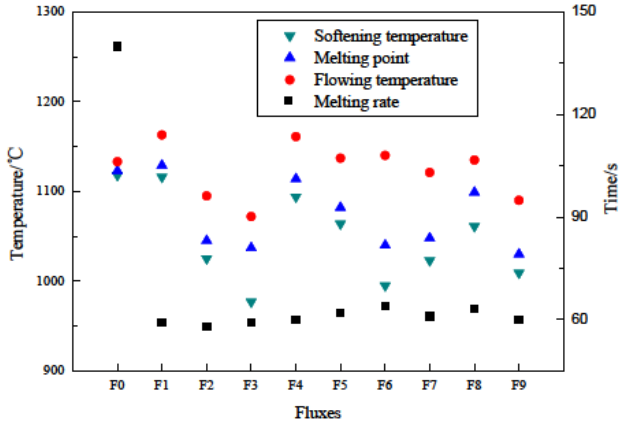

Figure 11: The melting temperature of fluxes 0 through 10

3.3 The melting characteristic

Figure 11 showed the results of softening temperature, melting point, flowing temperature and melting rate of mold fluxes were from the automatic tester slag melting point and melting speed.

The softening temperature of the original mold flux was 1118°C, the melting point was 1123°C, the flowing temperature was 1233°C and the melting rate was 140s. The softening temperature range of nine groups newly designed mold flux was from 977°C to 1116°C, the melting point range was from 1030°C to 1129°C, the flowing temperature range was from 1072°C to 1163°C, and the melting rate range was from 58 s to 64 s.

With the content of MgO, Na_2O and CaF_2 increased, the softening temperature, melting point and liquidus temperature [36] of the mold flux show a decreasing trend by comparing the melting temperatures of F0, F1, F2 and F3 groups with basicity of 0.9. The function of MgO, Na_2O, CaF_2 which could decrease the melting temperature was agreed with the basicity of 1.0 and 1.1.

R1, R2 and R3 represented respectively the basicity of 0.9, 1.0 and 1.1, N1, N2, N3 represented respectively the 6%, 8% and 10% content of Na_2O, M1, M2, M3 represented respectively the 1%, 2%, 3% content of MgO, C1, C2 and C3 represented respectively the 8%, 9% and 10% content of CaF_2. The melting point sequence was $H_{R3}>H_{R2}>H_{R1}$, $H_{N1}>H_{N2}>H_{N3}$, $H_{M1}>H_{M2}>H_{M3}$, $H_{C1}>H_{C2}>H_{C3}$ by means of weighted average calculation of melting temperatures of different groups. The results showed that the melting point of mold flux increased with the increase of basicity, while both Na_2O, MgO and CaF_2 could decrease the melting point.

The average melting rate of F1~F9 was about 60 s, but F0 was 140s. The results showed that the melting rate of mold flux decreased obviously with the carbon content increased.

3.4 The viscosity characteristic

Figure 12 showed the testing results of the viscosity of mold fluxes were from the Brookfield Rotary Viscometer.

The viscosity of original mold flux was 0.73 Pa·s at the temperature of 1300°C. The viscosity of nine groups newly designed mold flux range were from 0.33 Pa·s to 0.50 Pa·s at the temperature of 1300°C.

The viscosity sequence was $\eta_{R1}>\eta_{R2}>\eta_{R3}$ by means of weighted average calculation of the viscosity of mold fluxes with different basicity. The result showed that the viscosity of mold flux decreased with the basicity increased. Figure 13 showed the reaction process between CaO and chain-like silico-oxygen tetrahedron, the O^{2-}

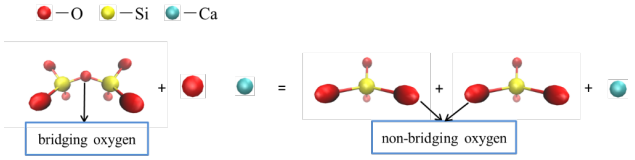

Figure 13: The reaction process of CaO and chain-like silico-oxygen tetrahedron

coming from CaO could replace the bridging oxygen in chain-like silico-oxygen tetrahedron, which was called non-bridging oxygen, and it could make the chain-like structure turn to sample. The number of non-bridging oxygen and the oxygen-silicon ratio increased when the basicity, the content of MgO and Na_2O increased, so the viscosity was decreased. There were two distinct models for the role of CaF_2 in silicate network structure [37], one was the Bills models, which held that CaF_2 was mainly used as diluent and not involved in breaking bridge oxygen. The other was Geist models, which suggested that CaF_2 was used as network modifier. Some researches [38–43] suggested that Si-F bond was formed by replaced the O atom of the Si-O bond. However, Sasaki *et al.* [44] and Gao *et al.* [45] found that Si-F bond could not form in the Na_2O-NaF-SiO_2 slag system. Mills [46] thought that CaF_2 was only used as diluent to decreased the viscosity. Persson and Seetharaman [47] suggested that CaF_2 was used as network modifier in the acid silicate slag and worked as diluent in the alkaline silicate slag. Regardless of the role of CaF_2, it could decrease the viscosity of mold flux.

The viscosity sequence was $\eta_{M1}>\eta_{M2}>\eta_{M3}$, $\eta_{N1}>\eta_{N2}>\eta_{N3}$ and $\eta_{C1}>\eta_{C2}>\eta_{C3}$ by means of weighted average calculation of the viscosity of different groups. The results showed that MgO, Na_2O and CaF_2 could reduce the viscosity as same as the FactSage simulated results. In terms of the effective of decreasing viscosity, the CaF_2 was better than the Na_2O, and the MgO was the last.

3.5 The crystallization characteristic

Figure 14 showed the crystallization temperature and crystalline fraction of ten groups mold flux by the SHTT/DHTT.

The crystalline fraction sequence was R3>R2>R1 by means of weighted average calculation of the crystalline fraction of different groups mold flux, which illustrated that increasing basicity of mold flux was beneficial to crystalline.

The crystallization temperature of F0 was 1045°C, and the strand shell temperature located at the outlet of mold

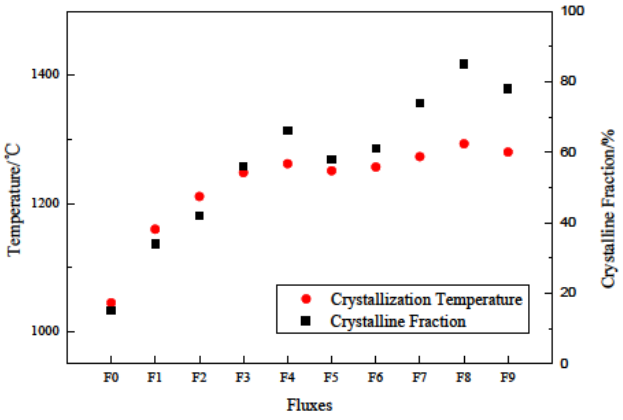

Figure 14: The crystallization temperature and crystalline fraction of mold flux

was about 1100°C [30], it meant that there was no liquid slag film which resulted the poor lubrication effect. The effective of heat-transfer control was bad because of its crystalline fraction was 15%. If it was applied to the production of peritectic steel, the surface longitudinal crack was easy to happen. The crystallization temperature range of F1~F9 were over 1100°C. The crystalline fraction of F1 and F2 were 34% and 42%, which were relative low resulting in the unsatisfactory effect of heat-transfer control. The crystalline fraction range of F3~F9 was from 56% to 85%, they not only ensured the lubrication function, but controlled effectively the horizontal heat-transfer of initial strand shell, which was benefit for the surface quality.

4 Application Effect

The production process of the Ti-bearing welding wire steel ER80-G was that: 120 t converter – LF refining – the continuous casting. The size of strand was 165 mm × 165 mm, the casting speed was 1.7 m/min, the mold taper was 0.87%/m, the casting temperature was among 1530°C~1560°C. The mold flux F0, F3, F5 and F9 were applied to the production of Ti-bearing welding wire steel ER80-G. Figure 15 showed the original morphology of strand surface using different mold fluxes.

There were transverse depression with equal spacing, longitudinal depression of different length, slag pit, slag runner appearing on the strand surface when the mold flux F0 was used in the production of Ti-bearing welding wire steel ER80-G. The poor strand surface quality was closely related to the mold flux F0. The melting rate, 140 s, was slow, the melting point, 1123°C, was normal, so the liquid slag layer became thinner resulting of it flowing into

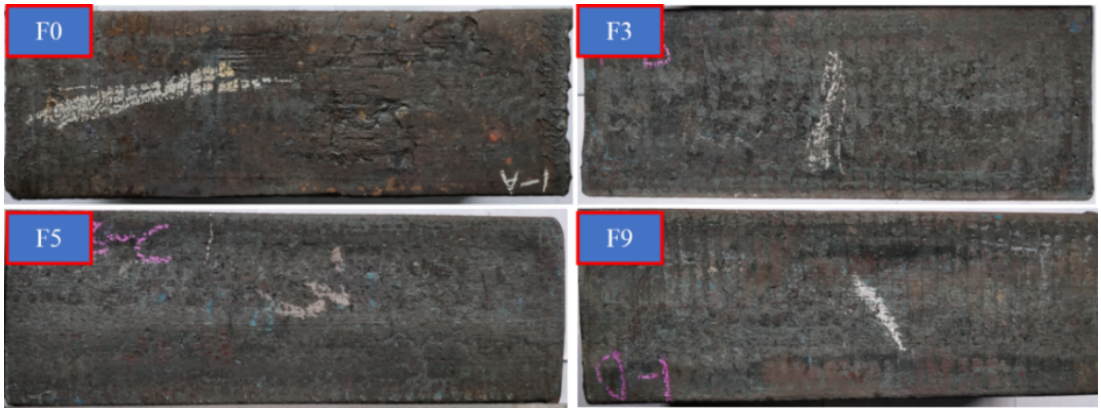

Figure 15: The original morphology of strand surface

the gap which located between the mold wall and initial strand shell could not be replenished in time. So the sintered layer was easier to flow into the gap when the mold oscillated, and the powdered slag layer may be also flowed into the gap together, resulting in the increase of friction between the initial strand shell and the mold wall, and then the slag runner and the slag pit were easy to appear. The viscosity, 0.73 Pa·s, was relatively high, resulting in the poor fluidity of the liquid slag layer and the non-homogeneous of liquid slag film, and then the heat-transfer of strand shell was non-uniform, which was easy to cause the surface depression and longitudinal crack for the Ti-bearing welding wire steel ER80-G with peritectic reaction.

The strand surface defects including transverse depression, longitudinal depression, slag pit and irregular oscillation mark were obviously improved when the newly design mold flux F3, F5, F9 were used to the production respectively. It suggested that the different basicity newly designed mold flux were beneficial to the strand surface quality.

5 Conclusions

The new mold flux was designed for the Ti-bearing welding wire steel ER80-G according to the solidification characteristics and slag system isothermal section diagram simulated by the FactSage thermodynamics software. The melting characteristic, viscosity characteristic and crystallization characteristic of the original mold flux and new designed mold flux had investigated by the automatic tester slag melting point and melting speed, the Brookfield rotary viscometer and SHTT/DHTT, and the specific conclusions were summarized as follows.

1. The liquidus temperature of Ti-bearing welding wire steel ER80-G was about 1513°C,and the solidification mode was $L\rightarrow L+\delta\rightarrow L+\gamma+\delta\rightarrow L+\gamma\rightarrow \gamma$. The peritectic reaction was occurred during the solidification process.
2. The initial melting temperature of the original mold flux was 1118°C, the melting point was 1123°C, the complete melting temperature was 1233°C and the melting rate was 140 s. The initial melting temperature range of nine groups newly designed mold flux was from 977°C to 1116°C, the melting point range was from 1030°C to 1129°C, the complete melting temperature range was from 1072°C to 1163°C, and the melting rate range was 58 s to 64 s. The melting point was increased with the basicity increased, but contrary to the content of MgO, Na_2O and CaF_2 increased. This relationship was the same as the FactSage simulated results.
3. The viscosity of original mold flux was 0.73 Pa·s at the temperature of 1300°C, and the viscosity of nine groups newly designed mold flux range was from 0.33 Pa·s to 0.50 Pa·s. It suggested that the basicity, MgO, Na_2O and CaF_2 could decrease the viscosity.
4. The crystallization temperature of the original mold flux was 1045°C, and the crystalline fraction was 15%. The original mold flux with the poor heat-transfer control and the bad lubrication effect was disadvantage for the production of peritectic steel ER80-G. The crystallization temperature range for nine groups newly designed mold flux was from 1160°C to 1293°C, the crystalline fraction range was from 34% to 85%. The crystalline fraction of F1 and F2 were relative low, which could not effectively control heat-transfer, but the newly design mold flux F3~F9 were better than F1 and F2 in heat-transfer control aspect.

5. There were a lot of transverse depression, longitudinal depression of different length, slag pit and slag runner appearing on the strand surface when the mold flux F0 was used in the production of Ti-bearing welding wire steel ER80-G. but the transverse depression, longitudinal depression and slag pit were reduced obviously when used the newly designed mold flux, it was proved that the newly designed mold flux could improve the strand surface quality of Ti-bearing welding wire steel ER80-G significantly.
6. In summary, the component content of mold flux for Ti-bearing welding wire steel ER80-G was suggested that the content of CaO was 28.4%, the content of SiO_2 was 31.6%, the basicity was 0.9, the content of MgO was 3%, the content of Na_2O was 10%, the content of CaF_2 was 10%, the content of Al_2O_3 was 6% and the content of Fe_2O_3 was 1%. The carbon material whose content was 10% was made up graphite and carbon black, and the ratio of them was 2:1. And the newly design mold flux all met the requirements when the basicity was 1.0 and 1.1.

Acknowledgement: The authors gratefully express their appreciation to the National Natural Science Foundation of China (51404088 and 51774141) and the Natural Science Foundation of Hebei Province of China (E2015209217) for sponsoring this work.

References

[1] Z.Y. Si, Z.Q. Wang, and P. Liu, J. Mater. Sci. Technol., 8 (1992) 294-297.
[2] J. Yang, J. Xue, and L.Y. Duan, J. Xi'an Jiaotong Univ., 33 (1999) 97-101.
[3] J. B. Chang, D. G. Ma, and S. W Li, Steelmak., 29 (2013) 62-66.
[4] J. B. Chang, D. G. Ma, and S. G. Li, Iron Steel, 48 (2013) 27-31.
[5] F. Xie, W. Q. Chen, and Y. W. Wang, Heat. Treat. Metals, 41 (2016) 100-103.
[6] W. S. Li, B. G. Tang, 12th China Welding Conference Paper, China, Hefei (2008), pp.1-12.
[7] T. Chen. A production method of high titanium alloy welding wire steel for billet continuous casting: China, 200910076071.9
[8] , 2009-06-17.
[9] S. Deng, J. C. Ma, W. J. Zhao, Iron Steel., 50 (2015) 32-37.
[10] Y. J. Yang, Special Steel, 36 (2015) 13-15.
[11] S Li, Y. X. Sun, H. C. Zhang, Henan Metall., 25 (2017) 13-15.
[12] H. G. Zheng, W. Q. Chen, and H. Chen, Special Steel, 25 (2004) 50-52.
[13] Z. Wang, Q. F. Shu, X. M. Hou, and K. C. Chou, Ironmak. Steelmak., 12 (2013) 210-215.
[14] Z. Q. Hao, W. Q. Chen, and C. Lippold, Metall. Mater. Trans. B., 41 (2010) 805-812.
[15] J. A. Bothma and P. C. Pistoriun, Ironmak. Steelmak., 34 (2007) 513-520.
[16] L. Liao and R.J. Fruehan, Ironmak. Steelmak., 16 (1989) 91-97.
[17] T. Mukongo, P. C. Pistorius, and A. M. Garbers-Craig, Ironmak, Steelmak., 31 (2004) 135-143.
[18] S. X. Zheng, Study on the dynamics of slag metal interfacial reaction in continuous casting mold for titanium bearing ferrite stainless steel, PhD thesis, Northeastern University, China, (2010).
[19] L. G. Zhu, X. J. Wang, Theories and application of continuous casting mold fluxes, Metallurgical Industry Press, Beijing, (2015).
[20] B. Xie, Y. N. Gan, and J. F. Wu, J. Iron Steel Res., 2 (1990) 5-12.
[21] K. L. S. Assis and P. C. Pistorius, Ironmak. Steelmak., 45 (2018) 502-508.
[22] K. Z. Gu, W. L. Wang, and J. Wei, H. Matsuura, Metall. Mater. Trans. B, 43 (2012) 1393-1404.
[23] L. L. Zhu, Q. Wang, and Q. Q. Wang, S. D. Zhang, and S. P. He, Ironmak. Steelmak., (2018), DOI: 10.1080/03019233.2018.1552773.
[24] F. Yang, Y. H. Han, and L. G. Zhu, Ironmak. Steelmak., (2018), DOI: 10.1080/03019233.2018.1516937.
[25] W. Yan, W. Q. Chen, Y. D. Yang and A. McLean, Ironmak. Steelmak., 46(4) (2019), 347-352.
[26] J. A. Bothma and P. C. Pistorius. Ironmak. Steelmak., 34 (2013) 513-520.
[27] Z. Q. Cui, Y. C. Tan, Metallography and Heat Treatment, Harbin Institute of Technology, Harbin, (2007).
[28] M. Hanao, M. Kawamoto, and A. Yamanaka, ISIJ Int., 52 (2012) 1310-1319.
[29] M. Kawamoto, Y. Tsukaguchi, and N. Nishida, ISIJ Int, 37 (1997) 134-139.
[30] P. C. Xiao, L. G. Zhu, X. J. Wang, Steelmak., 33 (2017) 56-62.
[31] X. Long, S. P. He, J. F. Xu, X. L. Huo, and Q. Wang, J. Iron Steel Res. Int., 19 (2012) 39-45.
[32] H. M. Wang, L. L. Yang, and G. R. Li, J. Iron Steel Res. Int., 20 (2013) 21-24.
[33] H. Wang, P. Tang, and G. H. Wen, Chin. J. Pro. Engineer., 10 (2010) 905-910.
[34] E. F. Wei, Y. D. Yang, and C. L. Feng, I. D. Sommerville, A Mclean. J. Iron Steel Res. Int., 13 (2006) 22-26.
[35] R. Scheel and W. Korte. MPT., 6 (1987) 22-23.
[36] C. L. Yang and G. H. Wen, P. Steel Res. Int, 87 (2016) 880-889.
[37] T. Schulz, B. Lychatz, N. Haustein, Metall. Mater. Trans. B., 44 (2013) 317-327.
[38] W. G. SEO and F. Tsukihashi. ISIJ Int., 44 (2004) 1817-1825.
[39] J. H. Park, D. J. Min, and H. S. Song, Metall. Mater. Trans. B., 33 (2002) 723-729.
[40] Q. Gao, Y. Min, and C. J. Liu, J. Iron Steel Res. Int., 24 (2017) 1152-1158.
[41] Y. Sasaki, K. Ishii. ISIJ Int., 44 (2004) 660-664.
[42] Y. Sasaki, M. Iguchi, and M. Hino, ISIJ Int., 47 (2007) 643-647.
[43] T. Sasaki, T. Yagi, and M. Susa. Ironmak. Steelmak., 30 (2003) 396-398.
[44] Y. Sasaki and H. Urata, K. Ishii., ISIJ Int., 43 (2003) 1897-1903.
[45] J. Gao, G. Wen, Q. Liu, P. Tang, J Non-Cryst Solids, 409 (2015) 8-13.
[46] K. C. Mills. ISIJ Int., 56 (2016) 1-13.
[47] M. Persson and S. Seetharaman, ISIJ Int., 47 (2007) 1711-1717.